

Magnetoelectric effect in composite structures based on ferroelectric–ferromagnetic perovskites

S.A. Solopan^a, O.I. V'yunov^{a,*}, A.G. Belous^a, A.I. Tovstolytkin^b, L.L. Kovalenko^a

^a Vernadskii Institute of General and Inorganic Chemistry, Ukrainian National Academy of Sciences, pr. Palladina 32/34, 03680 Kyiv, Ukraine

^b Institute of Magnetism, Ukrainian National Academy of Sciences, bul. Vernadskoho 36b, 03142 Kyiv, Ukraine

Available online 26 June 2009

Abstract

Composite structures based on ferroelectric $\text{BaTi}_{0.85}\text{Sn}_{0.15}\text{O}_3$ and $\text{Ba}_{0.996}\text{Y}_{0.004}\text{TiO}_3$ substrates and $\text{La}_{0.775}\text{Sr}_{0.225}\text{MnO}_3$ films deposited on them, which have a perovskite structure, have been prepared. The effect of different methods of film deposition on the properties of films has been studied. A detailed analysis and comparison of electrophysical properties and structure of ceramic and film ferromagnetics prepared by different methods has been carried out. The effect of the chemical composition of the substrate on the temperature of phase transition in manganite films has been studied. The possibility to control the magnetoresistivity of ferromagnetic films by electric field has been shown.

© 2009 Elsevier Ltd. All rights reserved.

Keywords: B. Composites; C. Electrical properties; C. Magnetic properties; D. BaTiO_3 and titanates; Manganites

1. Introduction

Recently, the interest in multiferroic and magnetoelectric materials considerably increased.^{1–3} This is accounted for by the discovery in 2001 of relatively high coefficients of magnetoelectric transformations in layered structures based on magnetostrictive $\text{Tb}_{1-x}\text{Dy}_x\text{Fe}_2$ and piezoelectric $\text{Pb}(\text{Zr,Ti})\text{O}_3$ materials.^{4,5} Later on, new methods for the preparation of complex composite structures and investigation of their properties have been developed. The possibility of their application as sensors of magnetic and electric fields,^{6,7} electric/magnetic field-controlled microwave filters,⁸ phase converters and delay networks,⁹ memory elements¹⁰ has also been shown.

It is known that ferroelectric and ferromagnetic substances in composite multiferroics may be coupled due to three different effects.¹¹ The first of them, the linear magnetoelectric effect is the induction of electric polarization by magnetic field or induction of magnetization by electric field. The second one, the effect of mutual magnetoelectric control is the switching of spontaneous polarization by magnetic field or spontaneous magnetization by electric field. And the third one, the effect of magnetocapacitance is the variation of permittivity by magnetic

field. The search for new types of coupling between ferroelectric and ferromagnetic substances in composite (multilayered) systems is of interest.

Therefore, the aim of the present work was the preparation of composite structures based on ferromagnetic $\text{La}_{0.775}\text{Sr}_{0.225}\text{MnO}_3$ films and ferroelectric substrates based on doped barium titanate, which have nonlinear electric properties ($\text{BaTi}_{1-x}\text{Sn}_x\text{O}_3$) and positive temperature coefficient of resistance (PTCR) ($\text{Ba}_{1-y}\text{Y}_y\text{TiO}_3$) and investigation of their magnetoresistance and crystal structure.

2. Experimental procedure

$\text{La}_{0.775}\text{Sr}_{0.225}\text{MnO}_3$ films were prepared by different methods: screen printing, magnetron sputtering and sol–gel method. At first, fine powder of this composition was prepared by sol–gel method and was used for sintering of ceramic samples.¹²

In the case of screen printing, synthesized $\text{La}_{0.775}\text{Sr}_{0.225}\text{MnO}_3$ powder and ethylene glycol as a solvent were used to prepare a homogeneous colloidal solution.¹³ This solution was deposited on substrates and heat treated at 800 °C for 2 h.

In the case of magnetron sputtering, films were deposited using a previously synthesized $\text{La}_{0.775}\text{Sr}_{0.225}\text{MnO}_3$ ceramic target and vacuum universal post VUP-5M.¹⁴ Films prepared were heat treated at 800 °C for 2 h.

* Corresponding author. Tel.: +380 44 4242211; fax: +380 44 4242211.
E-mail address: vyunov@ionc.kiev.ua (O.I. V'yunov).

Table 1
Unit-cell parameters of bulk samples.

Composition	Sp. gr.	Z	<i>a</i> , Å	<i>c</i> , Å	<i>V</i> , Å ³	<i>G</i> [<i>h k l</i>]
La _{0.775} Sr _{0.225} MnO ₃	<i>R</i> $\bar{3}c$	6	5.502(4)	13.349(6)	350.0 (4)	0
α -Al ₂ O ₃	<i>R</i> $\bar{3}c$	6	4.754(1)	12.982(1)	254.1 (1)	1.61 [00 1]
Ba _{0.996} Y _{0.004} TiO ₃	<i>P4mm</i>	1	3.9969(2)	4.0341(3)	64.448(8)	1.17 [1 1 0]
BaTi _{0.85} Sn _{0.15} O ₃	<i>P4mm</i>	1	4.0304(2)	4.0368(3)	65.576(6)	0.95 [1 1 0]

In the case of sol–gel method, previously synthesized La_{0.775}Sr_{0.225}MnO₃ ceramic samples were crushed into powder. This powder was dissolved in a mixture of HNO₃ and citric acid, then surface-active compound Triton X-100 was added. The solution was then heated in a boiling water bath to form a gel. The depositions were performed at 5400 rpm for 60 s two times using a spin coater SCI-20 (Novocontrol Technologies GmbH & Co. KG). The films were heated at a rate of 5 °C/min to a temperature of 1000 °C and annealed for 30 min.

A ceramic with nonlinear properties, BaTi_{0.85}Sn_{0.15}O₃,¹⁵ and with positive temperature coefficient of resistivity, Ba_{0.996}Y_{0.004}TiO₃ were used as substrates.¹⁶ Substrates based on α -Al₂O₃ (BK-100-1, Kineshma, Russia) were used for comparison.

X-ray powder diffraction (XRPD) measurements were performed on a DRON-4-07 powder diffractometer (Cu K α radiation, $2\theta = 10$ – 150°). Structure parameters were refined by Rietveld full profile analysis. The thickness of the films was determined by scanning electron microscopy (SEM) on a JEOL JCSA-733 SuperProbe. The electrical resistance of the films was measured by a four-probe technique in the temperature range from 77 to 350 K. Silver contacts were deposited by magnetron sputtering. Magnetoresistance (MR) was determined in applied fields of up to 1.2 MA/m using the equation $MR = (R_0 - R_H)/R_0 \times 100\%$, where R_0 is the zero-field resistance, and R_H is the resistance in magnetic field H .

3. Results and discussion

XRPD showed that the powder and ceramic La_{0.775}Sr_{0.225}MnO₃ samples used to prepare films were single-phase and had a rhombohedrally distorted perovskite structure, sp. gr. *R* $\bar{3}c$. The substrate materials were also single-phase and had a tetragonal perovskite structure, sp. gr. *P4mm* (BaTi_{0.85}Sn_{0.15}O₃, Ba_{0.996}Y_{0.004}TiO₃) or a rhombohedral structure, sp. gr. *R* $\bar{3}c$ (α -Al₂O₃). The substrates differ in lattice orientation: BaTi_{0.85}Sn_{0.15}O₃ and Ba_{0.996}Y_{0.004}TiO₃ are preferentially oriented in the [1 1 0] direction and α -Al₂O₃ is preferentially oriented in the [0 0 1] direction (Table 1).

XRPD showed (Fig. 1) that the La_{0.775}Sr_{0.225}MnO₃ films prepared using various methods and on various substrates were single-phase, but differed in lattice orientation. Curve 1 in Fig. 2 shows an XRPD pattern of ceramic La_{0.775}Sr_{0.225}MnO₃. The 1 1 0 and 1 0 4 reflections are seen to be close in intensity, which agrees with calculation. The La_{0.775}Sr_{0.225}MnO₃ film on Al₂O₃ substrates (scan 2) is [0 0 1]-oriented, which increases the intensity of reflection from (1 0 4) plane and planes close to it. In other systems (scans 3 and 4), the 1 1 0 reflection is stronger,

indicating (1 1 0) preferred orientation. The texturing factor indicates the presence of preferred orientation ($G \neq 0$, $G \neq 1$) or an orientation-disordered state of materials ($G = 0$, $G = 1$).¹⁷ It should be noted that preferred orientation is observed in all films prepared by different method.

Tables 1 and 2 list the Rietveld-refined structure parameters of La_{0.775}Sr_{0.225}MnO₃ ceramic and films, prepared by screen printing, magnetron sputtering and sol–gel method. To obtain accurate data, the parameters of both the film and substrate were simultaneously refined. It can be seen that the preferred orientation and unit cell parameters of the substrate influence both the preferred orientation and unit cell parameters of the film.

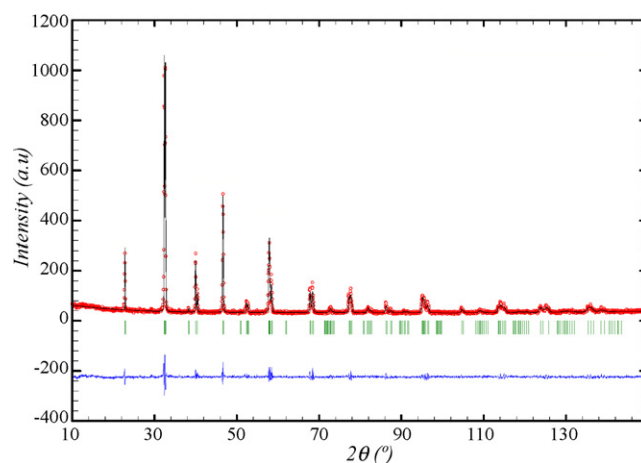


Fig. 1. Rietveld refinement of X-ray patterns of La_{0.775}Sr_{0.225}MnO₃ samples assuming the *R* $\bar{3}c$ sp. gr. The solid line is a fit of calculated to experimental data (crosses). Difference between measured and calculated intensities is given at the bottom. Bars correspond to Bragg peak positions.

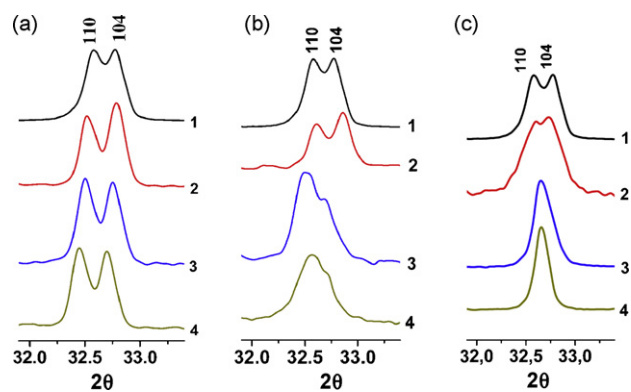


Fig. 2. XRPD patterns of La_{0.775}Sr_{0.225}MnO₃ as ceramic (1); as a film deposited on α -Al₂O₃ (2); Ba_{0.996}Y_{0.004}TiO₃ (3); BaTi_{0.85}Sn_{0.15}O₃ (4). Films were prepared by: (a) screen printing, (b) magnetron sputtering and (c) sol–gel method.

Table 2
Unit-cell parameters of $\text{La}_{0.775}\text{Sr}_{0.225}\text{MnO}_3$ films on different substrates.

Preparation method	Substrate composition	a , Å	c , Å	V , Å ³	G [hkl]
Screen printing	$\alpha\text{-Al}_2\text{O}_3$	5.5223(6)	13.3720(1)	353.16 (7)	0.15 [001]
	$\text{Ba}_{0.996}\text{Y}_{0.004}\text{TiO}_3$	5.5195(1)	13.3654(4)	352.63 (1)	0.14 [110]
	$\text{BaTi}_{0.85}\text{Sn}_{0.15}\text{O}_3$	5.5208(2)	13.3679(7)	352.86 (2)	0.11 [110]
Magnetron sputtering	$\alpha\text{-Al}_2\text{O}_3$	5.529(7)	13.37(1)	354.0(7)	1.40 [001]
	$\text{Ba}_{0.996}\text{Y}_{0.004}\text{TiO}_3$	5.5131(1)	13.3877(3)	352.40(1)	0.08 [110]
	$\text{BaTi}_{0.85}\text{Sn}_{0.15}\text{O}_3$	5.5110(1)	13.4089(9)	352.69(2)	0.23 [110]
Sol–gel	$\alpha\text{-Al}_2\text{O}_3$	5.523(1)	13.371(3)	353.26(1)	0.83 [001]
	$\text{Ba}_{0.996}\text{Y}_{0.004}\text{TiO}_3$	5.5217(4)	13.3685(6)	353.11(7)	0.21 [110]
	$\text{BaTi}_{0.85}\text{Sn}_{0.15}\text{O}_3$	5.5197(2)	13.3718(1)	352.85(4)	0.13 [110]

Increase in the structure parameters of the substrate increases those of the film. This may be due to the substrate surface determining the crystallographic direction of film crystallization.

The microstructure and thickness of the films was determined by electron microscopy (Fig. 3). The results indicate that screen-printed films have a porous structure and are 100 μm in thickness (Fig. 3a). The magnetron-sputtered films were dense and 500 nm in thickness. The grains of films had a columnar shape and a width of *ca.* 50 nm (Fig. 3b). In addition, a microscopic investigation of film surface was carried out. Sol–gel deposited films were 500 nm in thickness and had a grain size of *ca.* 100 nm (Fig. 3c).

Fig. 4 shows temperature dependences of normalized resistance for ceramic samples and films of $\text{La}_{0.775}\text{Sr}_{0.225}\text{MnO}_3$ prepared by different methods on various substrates. For the film on a $\alpha\text{-Al}_2\text{O}_3$ substrate (curve 2), the temperature maximum of resistance, T_{max} , is lower than that for ceramic $\text{La}_{0.775}\text{Sr}_{0.225}\text{MnO}_3$ (curve 1). At the same time, the maximum of the resistance of the films on $\text{BaTi}_{0.85}\text{Sn}_{0.15}\text{O}_3$ and $\text{Ba}_{0.996}\text{Y}_{0.004}\text{TiO}_3$ substrates shifts toward higher temperatures in comparison with the ceramic sample (curves 3 and 4). This effect can be understood in terms of preferred orientation of the films relative to the substrate.¹⁸

Fig. 5 shows temperature dependences of magnetoresistance in an applied field $H = 1.2 \text{ MA/m}$ for ceramic and film $\text{La}_{0.775}\text{Sr}_{0.225}\text{MnO}_3$ samples, prepared by different methods. It is known that the magnetoresistance of single-crystal manganites has a maximum near “metallic ferromagnet–dielectric paramagnet” transition (Curie temperature T_C).^{19,20} In polycrystalline samples, an additional contribution to MR arises

at low temperatures ($T < T_C$), which increases with decreasing temperature. This contribution arises due to spin-dependent scattering¹⁹ or to spin-polarized tunneling²¹ of charge carriers at grain boundaries.

Two contributions to magnetoresistance are clearly distinguished for $\text{La}_{0.775}\text{Sr}_{0.225}\text{MnO}_3$ both as ceramic and as films deposited on doped barium titanate substrates (Fig. 5, curves 1, 3 and 4). This allows the T_C of these samples to be determined as the temperature of maximum on the $\text{MR}(T)$ curve. The temperature dependence of MR for film on $\alpha\text{-Al}_2\text{O}_3$ substrate is typical of inhomogeneous or strained manganites, which are characterized by a diffuse phase transition.²¹ It should be noted that similar dependences are observed for all $\text{La}_{0.775}\text{Sr}_{0.225}\text{MnO}_3$ films prepared by different methods on $\alpha\text{-Al}_2\text{O}_3$ substrate. Thus, the present results demonstrate that the films produced on $\alpha\text{-Al}_2\text{O}_3$ and doped barium titanate substrates differ in phase transition temperature, which is associated with the difference in the preferred orientation of the films relative to the substrate.²²

Fig. 6 shows a composite structure based on $\text{La}_{0.775}\text{Sr}_{0.225}\text{MnO}_3$ film which, was used to study the effect of the properties of substrates on the properties of ferromagnetic material. The electrical resistance and magnetoresistance of the films was determined using electrodes 4 and 5. A voltage was applied between the electrodes 2 and 3 or between the electrode 1 and short-circuited electrodes 2 and 3. The measurements were made in an applied magnetic and/or electric field or in zero field.

The investigations showed that the properties of PTCR $\text{Ba}_{0.996}\text{Y}_{0.004}\text{TiO}_3$ substrate affect the properties of magnetic film. Fig. 7 shows an example of the temperature dependence

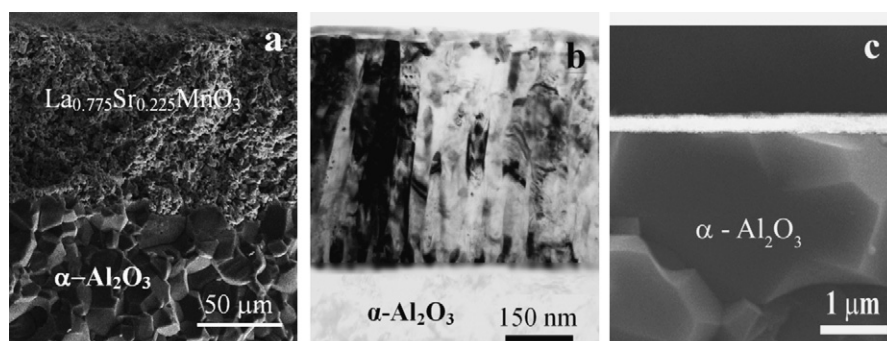


Fig. 3. SEM pictures of $\text{La}_{0.775}\text{Sr}_{0.225}\text{MnO}_3$ films deposited on $\alpha\text{-Al}_2\text{O}_3$ substrate by: (a) screen printing, (b) magnetron sputtering and (c) sol–gel method.

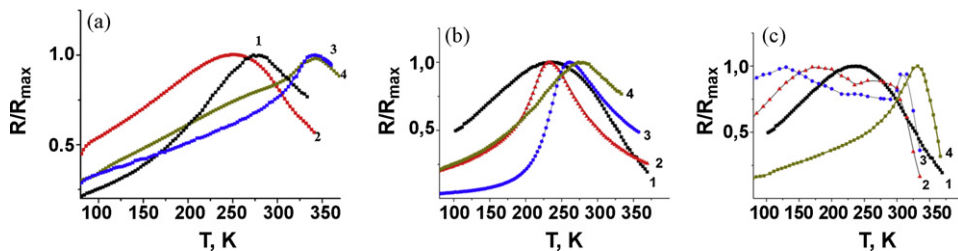


Fig. 4. Temperature dependences of normalized resistance for a bulk $\text{La}_{0.775}\text{Sr}_{0.225}\text{MnO}_3$ sample (1), $\text{La}_{0.775}\text{Sr}_{0.225}\text{MnO}_3$ films on $\alpha\text{-Al}_2\text{O}_3$ (2), $\text{Ba}_{0.996}\text{Y}_{0.004}\text{TiO}_3$ (3) and $\text{BaTi}_{0.85}\text{Sn}_{0.15}\text{O}_3$ (4) deposited by: (a) screen printing, (b) magnetron sputtering and (c) sol–gel method.

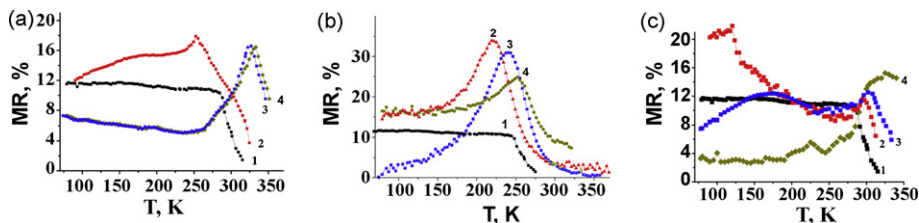


Fig. 5. Temperature dependences of magnetoresistance for a bulk $\text{La}_{0.775}\text{Sr}_{0.225}\text{MnO}_3$ sample (1), $\text{La}_{0.775}\text{Sr}_{0.225}\text{MnO}_3$ films on $\alpha\text{-Al}_2\text{O}_3$ (2), $\text{Ba}_{0.996}\text{Y}_{0.004}\text{TiO}_3$ (3) and $\text{BaTi}_{0.85}\text{Sn}_{0.15}\text{O}_3$ (4); (a) screen printing; (b) magnetron sputtering; (c) sol–gel method.

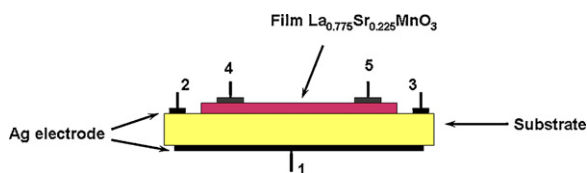


Fig. 6. Composite structure based on $\text{La}_{0.775}\text{Sr}_{0.225}\text{MnO}_3$ films (red) on various substrates (yellow); (1)–(5) are electrodes. (For interpretation of the references to color in this figure legend, the reader is referred to the web version of the article.)

of the electrical resistance of $\text{La}_{0.775}\text{Sr}_{0.225}\text{MnO}_3$ film on a $\text{Ba}_{0.996}\text{Y}_{0.004}\text{TiO}_3$ substrate for different applied external electric fields. At zero voltage or a voltage applied between the electrodes 2 and 3, the slope of the $R(T)$ curve changes sharply near the phase transition (curves 2 and 3). A voltage applied between the electrodes 1 and 2 (curve 1) shifts the phase transition and reduces the resistance of the film. This behavior can

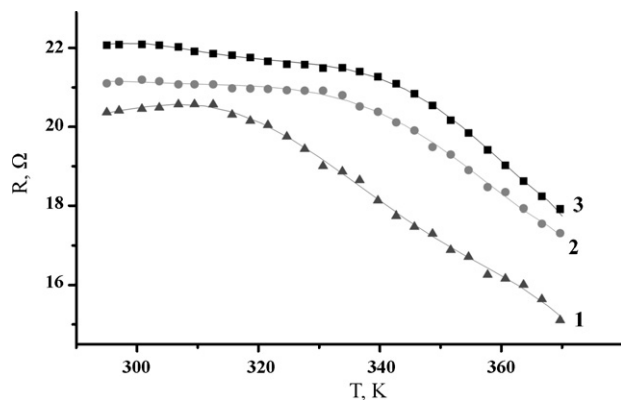


Fig. 7. Resistance as a function of temperature for a $\text{La}_{0.775}\text{Sr}_{0.225}\text{MnO}_3$ film on a $\text{Ba}_{0.996}\text{Y}_{0.004}\text{TiO}_3$ substrate at 30 V voltage applied between the electrodes 1 and 2 (1), between the electrodes 2 and 3 (2) and at zero voltage (3).

be accounted for by the sensitivity of doped PTCR barium titanate to external electric field and by magnetoelectric coupling between the layers.

Fig. 8 shows temperature dependences of the resistance of $\text{La}_{0.775}\text{Sr}_{0.225}\text{MnO}_3$ film on a $\text{Ba}_{0.996}\text{Y}_{0.004}\text{TiO}_3$ substrate in applied electric and magnetic fields. Fig. 8 demonstrates that the resistance of film is not changed by external electric field applied to the substrate, but decreases by the action of external magnetic field (curves 1 and 2) due to magnetoresistive effect.²¹

The investigations showed that in contrast to above-mentioned composite structure, there is no coupling between magnetoelectric and ferroelectric substances in composite structures based on magnetoelectric $\text{La}_{0.775}\text{Sr}_{0.225}\text{MnO}_3$ film on a ferroelectric doped barium titanate substrate with nonlinear properties, $\text{BaTi}_{1-x}\text{Sn}_x\text{O}_3$.

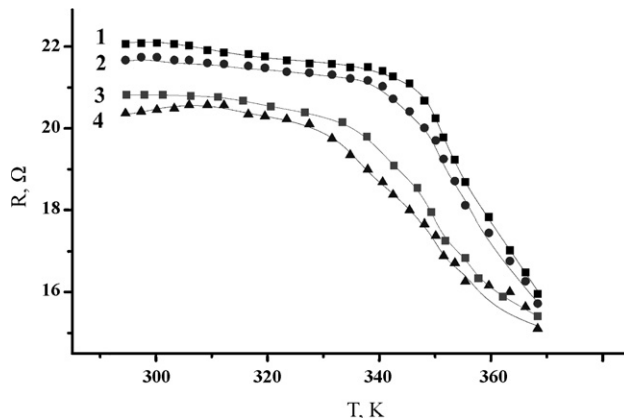


Fig. 8. Resistance as a function of temperature for a $\text{La}_{0.775}\text{Sr}_{0.225}\text{MnO}_3$ film on a $\text{Ba}_{0.996}\text{Y}_{0.004}\text{TiO}_3$ substrate in applied electric and magnetic fields: $H = 1.2 \text{ MA/m}$, $V = 0$ (1); $H = 1.2 \text{ MA/m}$, $V = 20 \text{ V}$ (2); $H = 0$, $V = 0$ (3); $H = 0$, $V = 20 \text{ V}$ (4).

4. Conclusions

The results of investigations allow two-layer structures to be prepared, which consist of ferromagnetic $\text{La}_{0.775}\text{Sr}_{0.225}\text{MnO}_3$ films on ferroelectric doped barium titanate substrates with nonlinear properties ($\text{BaTi}_{0.85}\text{Sn}_{0.15}\text{O}_3$) or with positive temperature coefficient of resistance ($\text{Ba}_{0.996}\text{Y}_{0.004}\text{TiO}_3$). It has been shown that preferred orientation and unit cell parameters of substrates affect greatly the properties of deposited ferromagnetic films. It has been found that ferroelectric and ferromagnetic substances in composite structure can be coupled due to PTCR effect in ferroelectric phase.

Acknowledgement

The authors would like to acknowledge the financial support from the Science and Technology Center in Ukraine (under project # 4020).

References

1. Ramesh, R. and Spaldin, N. A., Multiferroics: progress and prospects in thin films. *Nat. Mater.*, 2007, **6**, 21–29.
2. Schmid, H., Multiferroic magnetoelectrics. *Ferroelectrics*, 1994, **162**, 665–685.
3. Eerenstein, W., Mathur, N. D. and Scott, J. F., Multiferroic and magnetoelectric materials. *Nature*, 2006, **442**, 759–765.
4. Jungho, R., Shashank, P., Carazo, A. V. and Uchino, K., Effect of the magnetostrictive layer on magnetoelectric properties in lead zirconate titanate/terfenol-D laminate composites. *J. Am. Ceram. Soc.*, 2001, **84**, 2905–2908.
5. Dong, S., Jie-Fang, Li. and Viehland, D., Ultrahigh magnetic field sensitivity in laminates of TERFENOL-D and $\text{Pb}(\text{Mg}_{1/3}\text{Nb}_{2/3})\text{O}_3$ – PbTiO_3 crystals. *Appl. Phys. Lett.*, 2003, **83**, 2265–2267.
6. Dong, S., Zhai, J., Xing, Z., Jie-Fang, Li. and Viehland, D., Extremely low frequency response of magnetoelectric multilayer composites. *Appl. Phys. Lett.*, 2005, **86**, 102901–102903.
7. Dong, S., John, G. B., Zhai, J., Jie-Fang, Li., Lu, G. Q., Viehland, D. et al., Circumferential-mode, quasi-ring-type, magnetoelectric laminate composite—a highly sensitive electric current and/or vortex magnetic field sensor. *Appl. Phys. Lett.*, 2005, **86**, 182506–182508.
8. Srinivasan, G., Tatarenko, A. S. and Bichurin, M. I., Electrically tunable microwave filters based on ferromagnetic resonance in ferrite-ferroelectric bilayers. *Electron. Lett.*, 2005, **41**, 596–598.
9. Fetisov, Y. K. and Srinivasan, G., Electric field tuning characteristics of a ferrite-piezoelectric microwave resonator. *Appl. Phys. Lett.*, 2006, **88**, 143503–143505.
10. Scott, J. F. and Paz de Araujo, C. A., Ferroelectric memories. *Science*, 1989, **246**, 1400–1405.
11. Nan, Ce-Wen., Bichurin, M. I., Dong, S., Viehland, D. and Srinivasan, G., Multiferroic magnetoelectric composites: historical perspective, status, and future directions. *J. Appl. Phys.*, 2008, **103**, 031101–031136.
12. Belous, A. G., V'yunov, O. I., Pashkova, E. V., Yanchevskii, O. Z., Tovstolytkin, A. I. and Pogorelii, A. M., Effect of chemical content and sintering temperature on the structure of solid solution $\text{La}_{1-x}\text{Sr}_x\text{MnO}_{3+y}$. *Inorg. Mater.*, 2003, **39**, 212–222.
13. Dutronc, P., Carbonne, B., Mienil, F. and Lucat, C., Influence of the nature of the screen-printed electrode metal on the transport properties of thick-film semiconductor gas sensors. *Sens. Actuators B*, 1992, **6**, 279–284.
14. Tovstolytkin, A. I., Pogorily, A. N., Matviyenko, A. I., Vovk, A. Y. and Wang, Z., Discrete deposition as a powerful tool to govern magnetoresistance of the doped manganite films. *J. Appl. Phys.*, 2005, **98**, 043902–043907.
15. Solopan, S. A., Belous, A. G., V'yunov, O. I. and Kovalenko, L. L., $\text{BaTi}_{1-x}\text{Sn}_x\text{O}_3$ solid solutions: solid-phase and sol–gel syntheses and characterization. *Russ. J. Inorg. Chem.*, 2008, **53**, 157–163.
16. Belous, A. G., V'yunov, O. I. and Kovalenko, L. L., $(\text{Ba},\text{Y})(\text{Ti},\text{Zr},\text{Sn})\text{O}_3$ -based PTCR materials. *Ferroelectrics*, 2001, **254**, 91–99.
17. Rodríguez-Carvajal, J., In *An introduction to the program FullProf 2000*, 2001, pp. 54–55.
18. Chen, C.-C. and de Lozanne, A., Electronic transport properties of $(001)/(110)$ oriented $\text{La}_{2/3}\text{MnO}_{3-\delta}$ thin films. *Appl. Phys. Lett.*, 1998, **73**, 3950–3952.
19. Li, X. W., Gupta, A., Xiao, G. and Gong, G. Q., Low-field magnetoresistive properties of polycrystalline and epitaxial perovskite manganite films. *Appl. Phys. Lett.*, 1997, **71**, 1124–1126.
20. Ghosh, K., Ogale, S. B., Ramesh, R., Greene, R. L., Venkatesan, T., Gapchup, K. M. et al., Transition-element doping effects in $\text{La}_{0.7}\text{Ca}_{0.3}\text{MnO}_3$. *Phys. Rev. B*, 2000, **59**, 533–537.
21. Dorr, K., Ferromagnetic manganites: spin-polarized conduction versus competing interactions. *J. Phys. D: Appl. Phys.*, 2006, **39**, 125–150.
22. Nath, T. K., Rao, R. A., Lavric, D. and Eom, C. B., Effect of three-dimensional strain states on magnetic anisotropy of $\text{La}_{0.8}\text{Ca}_{0.2}\text{MnO}_3$ epitaxial thin films. *Appl. Phys. Lett.*, 1999, **74**, 1615–1617.